ARTICLE Communicated by Terrence Sejnowski

A Cerebellar Computational Mechanism for Delay Conditioning at Precise Time Intervals

Terence D. Sanger
terry@sangerlab.net
Departments of Biomedical Engineering, Neurology, and Biokinesiology, University of Southern California, Los Angeles, CA 90089, U.S.A.

Mitsuo Kawato
kawato@atr.jp
Brain Information Communication Research Laboratory Group, Advanced Telecommunications Research Institutes International, Kyoto 619-0288, Japan, and Center for Advanced Intelligence Project, RIKEN, Chuo-ku, Tokyo, 103-0027, Japan

The cerebellum is known to have an important role in sensing and execution of precise time intervals, but the mechanism by which arbitrary time intervals can be recognized and replicated with high precision is unknown. We propose a computational model in which precise time intervals can be identified from the pattern of individual spike activity in a population of parallel fibers in the cerebellar cortex. The model depends on the presence of repeatable sequences of spikes in response to conditioned stimulus input. We emulate granule cells using a population of Izhikevich neuron approximations driven by random but repeatable mossy fiber input. We emulate long-term depression (LTD) and long-term potentiation (LTP) synaptic plasticity at the parallel fiber to Purkinje cell synapse. We simulate a delay conditioning paradigm with a conditioned stimulus (CS) presented to the mossy fibers and an unconditioned stimulus (US) some time later issued to the Purkinje cells as a teaching signal. We show that Purkinje cells rapidly adapt to decrease firing probability following onset of the CS only at the interval for which the US had occurred. We suggest that detection of replicable spike patterns provides an accurate and easily learned timing structure that could be an important mechanism for behaviors that require identification and production of precise time intervals.

1 Introduction

With the evolution of vertebrates came the problem of combination of sensory signals and coordination of motor commands that arrive from and are destined for distant parts of the body. Different body regions are connected to the central nervous system by neurons whose axons are responsible for

Neural Computation **32, 2069–2084** (2020)

https://doi.org/10.1162/neco_a_01318

differing delays in transmission. This creates the need for recognition and generation of signals with precise time delays. While some delays are determined by neuroanatomy and therefore unchanging, the need to interact with a dynamic environment requires the ability to learn and replicate arbitrary time intervals (Molinari, Leggio, & Thaut, 2007). This function is often attributed to the cerebellum (Bareš et al., 2019), and cerebellar injury impairs the estimation and production of millisecond-precision time intervals up to about 1 to 2 seconds in duration (Buhusi & Meck, 2005; Ivry & Spencer, 2004; Schwartze, Keller, & Kotz, 2016). A common experimental paradigm is eyeblink conditioning, in which a behaviorally irrelevant conditioned stimulus (CS) is repeatedly followed at a predictable interval by a puff of air on the cornea (unconditioned stimulus, US). After training, presentation of the CS without the US leads to an eyeblink at the precise interval at which the US would normally have occurred (Attwell, Ivarsson, Millar, & Yeo, 2002; Gerwig, Kolb, & Timmann, 2007; Kim & Thompson, 1997; Kotani, Kawahara, & Kirino, 2002; Raymond & Medina, 2018).

The mechanism by which time intervals can be learned and replicated is the subject of multiple models (Yamazaki & Tanaka, 2009). Proposed mechanisms include delays implemented by the time required for axonal conduction or conduction through neural circuits (Buonomano, 2003; Braitenberg, 1967), rhythmic pattern generators with a known period (Miall, 1989; Panzeri, Ince, Diamond, & Kayser, 2014), beat frequency between oscillators at differing frequencies (Buhusi & Meck, 2005), synchronized firing of groups of neurons (Hopfield & Brody, 2001), or superimposed time-varying waveforms that can be combined to produce temporal sequences (Medina, Garcia, Nores, Taylor, & Mauk, 2000; Narain, Remington, De Zeeuw, & Jazayeri, 2018). A particularly interesting group of models suggests that random but repeatable dynamics can be generated by feedback loops between granule cells and Golgi cells, and the resulting time-varying patterns triggered by the conditioned stimulus allow determination of time intervals (Roössert, Dean, & Porrill, 2015; Yamazaki & Tanaka, 2007a, 2007b). While most of these mechanisms are able to approximate smooth temporal sequences, they do not have the ability to learn a rapid eyeblink at an arbitrary time interval with millisecond precision because they are based on average firing rates rather than instantaneous spikes (Karmarkar & Buonomano, 2007). The precision, repeatability, and stability of rate-based models may not reflect the true challenges of achieving millisecond precision timing with interconnected populations of spiking neurons Even in a model based on simulation of populations of spiking neurons, time-varying patterns in granule cells are expressed as relatively slow variations in firing rates that cannot be identified at millisecond precision (Yamazaki & Tanaka, 2007b).

We propose a new mechanism for learning time intervals with millisecond precision. This mechanism is based on patterns of activity within populations of granule cells, but the patterns are determined by predictable and repeatable (although random-appearing) sequences of individual spikes

rather than by slower temporal patterns of spike rates, oscillations, or synchrony. The mechanism requires that cerebellar granule cells are able to produce nearly identical spike trains for similar inputs and that the Purkinje cells can recognize specific patterns in the population of granule cells. If these two conditions are met, then the pattern of spikes in the population provides a unique and precise time stamp at any desired time interval, and the association of a training signal in the climbing fibers at a particular time interval after the stimulus allows plasticity at the parallel fiber to Purkinje cell synapses to respond to the pattern of activity at that specific time. There is accumulating evidence that even though cell spike sequences appear to have Poisson statistics, they may not be random and often have the repeated sequences required for this mechanism (Alstrøm, Beierholm, Nielsen, Ryge, & Kiehn, 2002; Hires, Gutnisky, Yu, O'Connor, & Svoboda, 2015; Kayser, Logothetis, & Panzeri, 2010; Mainen & Sejnowski, 1995; Masquelier, 2013; Nolte, Reimann, King, Markram, & Muller, 2019; Petersen, Panzeri, & Diamond, 2001, 2002; Shmiel et al., 2005). This is consistent with theoretical results showing that for certain classes of nonlinear systems, apparently chaotic but nevertheless repeatable sequences can be achieved (Rössert et al., 2015; Uchida, McAllister, & Roy, 2004). Although this phenomenon has not yet been tested in granule cells, we suggest that the identification of time-stamped patterns of neural activity may provide a widespread mechanism for the representation of time intervals and the synchronization of events with repeatable time delays within the cerebellum, as well as elsewhere in the brain.

The model and simulations we propose we have here are intended to demonstrate the potential for this computational mechanism to generate and recognize precise time intervals in response to pairings of CS and US. Although this can be perhaps interpreted as a model for certain behavioral phenomena including eyeblink conditioning, we emphasize that we do not attempt to emulate many of the more complex and interesting behavioral phenomena associated with eyeblink or other conditioned reflexes, we do not attempt to match the empirically observed firing patterns of granule or Purkinje cells, and the time intervals we have chosen are intended for illustration rather than as a specific instance of conditioning. Our intent is to show in a very simplified model that there is a previously undescribed computational mechanism based on spike timing that has the potential to be used to generate time intervals and response patterns with millisecond precision after relatively short periods of training.

2 Methods

Cerebellar learning is simulated in Matlab, based on common connectivity and plasticity models (for review, see D'Angelo, 2014; Raymond & Medina, 2018). The network (see Figure 1) is constructed of 100 mossy fibers, 2000 granule cells, and a single output Purkinje cell. Each granule cell contacts

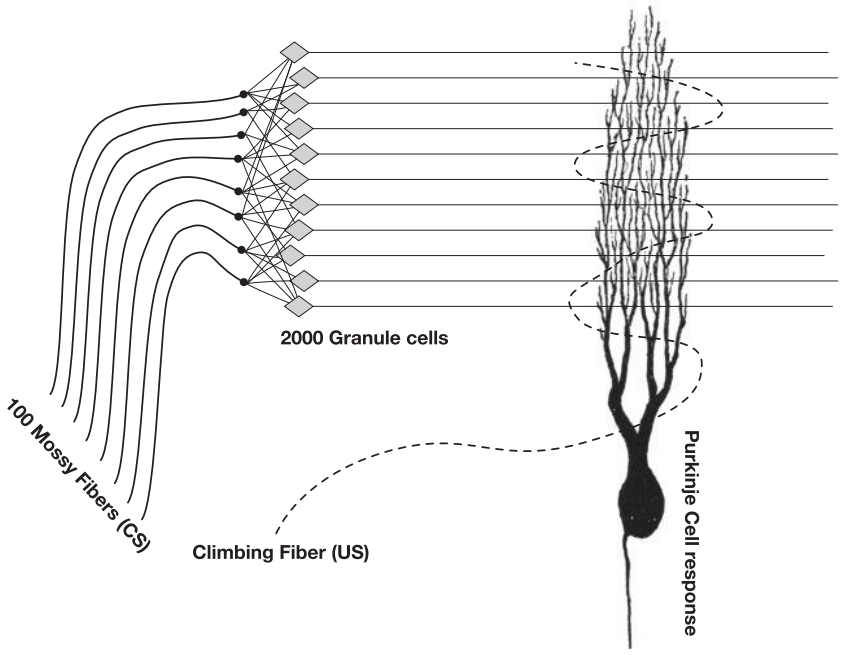

Figure 1: Structure of the simplified cerebellar model. The conditioned stimulus (CS) on 100 mossy fibers is expansion recoded onto 2000 granule cells, each of which takes input from four mossy fibers. The granule cell axons are the parallel fibers that contact the synapses of a Purkinje cell. The climbing fiber from a cell in the inferior olive contacts the Purkinje cell and supplies the unconditioned stimulus (US). The output of the Purkinje cell makes an inhibitory synapse with deep cerebellar nuclei.

four randomly selected mossy fibers via excitatory synapses, and the Purkinje cell contacts all granule cells via excitatory synapses. Granule cells do not synapse on other granule cells. Granule cell membrane potential and spike generation obey the Izhikevich approximation (Izhikevich, 2003) to the Hodgkin-Huxley equations integrated at 1 msec timescale, with parameters tuned as fast-spiking neurons ($a = 0.16$, $b = 0.225$, $c = -65$, $d = 8$) with 5% jitter of each parameter to simulate differences between cells.

We emulate a delay conditioning paradigm in which the conditioned stimulus (CS) and unconditioned stimulus (US) overlap in time. This is because in the absence of overlap (trace conditioning), the response may depend on other brain regions, including the hippocampus (Beylin et al., 2001; Kim, Clark, & Thompson, 1995; Weiss, Bouwmeester, Power, & Disterhoft, 1999), although more recent results suggest that trace and delay conditioning may share mechanisms at the Purkinje cell (Halverson, Khilkevich, &

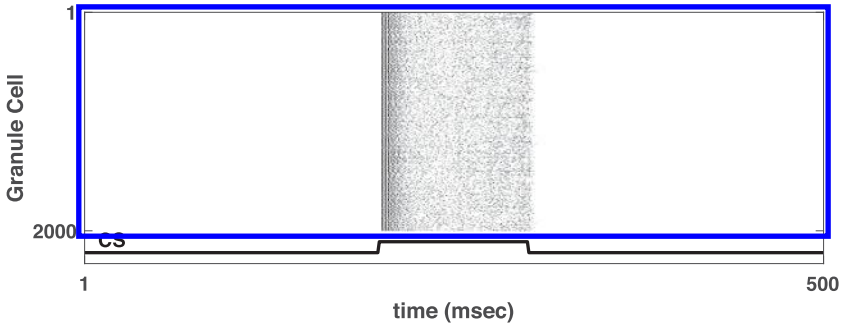

Figure 2: Pattern of granule cell firing during a single trial. Each row is the spikes for one of the 2000 granule cells. Cells only fire when driven by the mossy fiber inputs during the conditioned stimulus (CS), between 200 and 300 msec. The pattern repeats, and the intertrial interval is therefore 400 msec between the end of one CS and the start of the next.

Mauk, 2018). In our model as well as most other models that depend on temporal patterns of granule cell activity, in the absence of overlap between CS and US, the CS input drive from the mossy fibers to the granule cells is absent at the time of the US, so the parallel fibers to Purkinje cell synapses are not activated and learning cannot be performed.

The conditioned stimulus is presented for 100 msec, and the US is presented for 10 msec, starting 70 msec after the start of the CS. The US is indicated by climbing fiber input, and we represent this as a 10 msec constant signal. The CS is a set of 100 independent Poisson spike trains with average rate of 200 Hz, one for each of the 100 mossy fiber inputs. The same spike train pattern is given for each presentation of the CS. When the CS is not present, the mossy fibers are silent. Fifty trials are performed in sequence, each with the same pattern of spikes on the set of 100 incoming mossy fibers. Mossy fiber to granule cell synapses create a depolarizing excitatory postsynaptic current (EPSC) with 40 msec time constant and average amplitude of 10 microAmps with 10% random variation in the EPSC size between different synapses. The intertrial interval is 400 msec, which is sufficient for the Izhikevich granule cells to return to their fully resting state. Figure 2 shows an example of the pattern of granule cell firing for a single trial.

The granule cell to Purkinje cell synapses have a variable synaptic strength w_i indicated by a value between 0 and 1. The Purkinje cell excitatory postsynaptic potential is calculated at each 1 msec time step as

$$\text{EPSP} = \frac{1}{\sqrt{\sum_i g_i^2}} \sum_i w_i g_i, \tag{2.1}$$

where g_i is 1 if the ith granule cell fired and zero otherwise. Granule cell input is normalized by RMS input power (equivalently, $\sqrt{\sum_i g_i}$) because the relatively small number of granule cells in our simulation leads to much larger variance in the mean input than would be present in the biological system. The Purkinje cells fire with Poisson statistics such that firing rate is proportional to the EPSP, adjusted to have a maximum rate of 50 Hz. Golgi cells, stellate cells, basket cells, plasticity at the mossy fiber to granule cell synapse, and the effect of nitric oxide and catecholamines are not modeled.

Plasticity is simulated only at the granule cell to Purkinje cell synapses. Long-term potentiation (LTP) occurs by adding a value to the synaptic weight of 0.0001 per spike, whenever there is an incoming spike on a granule cell, independent of whether the Purkinje cell fires. This simulates the absence of backpropagating action potentials in the Purkinje cells, so that synapses are not aware of output firing and thus do not implement a true Hebbian-type learning rule. Long-term depression (LTD) occurs by subtracting a value of 0.03 per spike for each granule cell spike that occurs during the US. Since the US is assumed to trigger activity on climbing fibers, this simulates the LTD associated with coincident Purkinje cell complex spikes and incident granule cell firing. All weights w_i are maintained between 0 and 1. This algorithm can be written as

$$\Delta \mathbf{w}(t) = \mathbf{g} * ((1 - US(t)) * LTPrate - US(t) * LTDrate), \tag{2.2}$$

where $\mathbf{w} =< w_0 \ldots w_{2000} >$ is the synaptic vector of weights w_i, $\Delta \mathbf{w}(t)$ is the vector change in the weight at time step t, $\mathbf{g} =< g_0 \ldots g_{2000} >$ is a binary vector with $g_i = 1$ for every granule cell that fired, $US(t)$ is the scalar value of the unconditioned stimulus at time t, and *LTPrate* and *LTDrate* are scalars indicating the amounts of LTP or LTD that occur in response to a single spike event. Equation 2.2 operates continually from the start of the experiment to the end, reflecting changes in weights for every US event as these occur.

Equation 2.2 will drive the Purkinje cell output to zero during times that correspond to positive values of the unconditioned stimulus *US*. However, this same circuitry can be used to approximate desired smooth functions if instead we use the Widrow-Hoff LMS rule (Widrow & Hoff, 1960) for training:

$$\Delta \mathbf{w}(t) = LTDrate * \mathbf{g} * (1 - US(t) - PCoutput), \tag{2.3}$$

where *PCoutput* is the scalar probability of the Purkinje cell firing, approximated as proportional to the instantaneous magnitude of its membrane potential. In this case, the Purkinje cell output will converge through learning to approximate the time-varying signal $US(t)$.

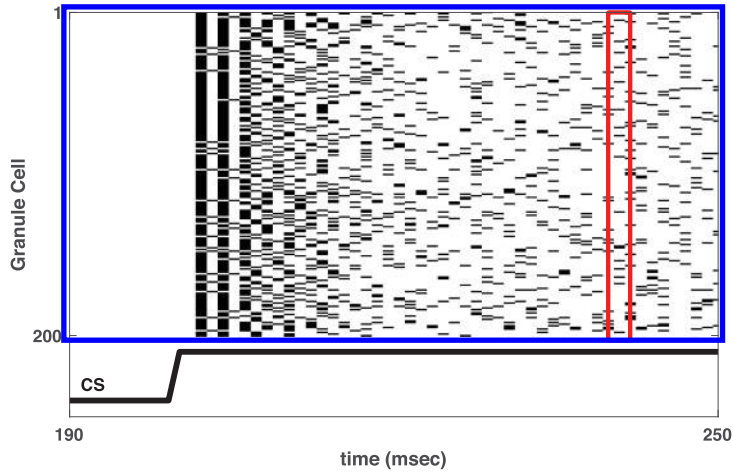

Figure 3: Demonstration of time interval recognition from the population pattern. Spike rasters from only 200 granule cells are shown during the first 50 msec of the conditioned stimulus (CS). The red box illustrates how a particular pattern of spikes can uniquely identify a particular time interval following the start of the CS.

Following training, the Purkinje cell EPSP is calculated using equation 2.1 while the CS is on but the US is inactive. Successful recognition of the pattern of granule inputs that had been present during the US will result in the Purkinje cell firing rate dropping to zero in the absence of the US whenever the selected pattern occurs (see Figure 3).

To estimate the probability that an untrained pattern could be mistaken for a pattern present during the US, we calculate the cross-correlation matrix between each different pattern. We compare the magnitude of the diagonal elements of the cross-correlation matrix (responding to the correct pattern) with the magnitude of the off-diagonal elements (responding to an incorrect pattern).

Because neither the granule cell to Purkinje cell synaptic weights nor the granule cell inputs can represent negative numbers, orthogonality of different granule cell patterns occurs only when there is no overlap between patterns. This substantially reduces the number of possible orthogonal patterns representable in any population. At least 2000 granule cells appear to be needed for reliable results in our simulation. Since those cells are driven by only 100 mossy fiber inputs, there needs to be a method to distribute the inputs randomly across the granule cells. Expansion coding is necessary in our simulation in order to allow a rich enough representation to achieve a unique pattern on the parallel fibers for each stimulus at each time.

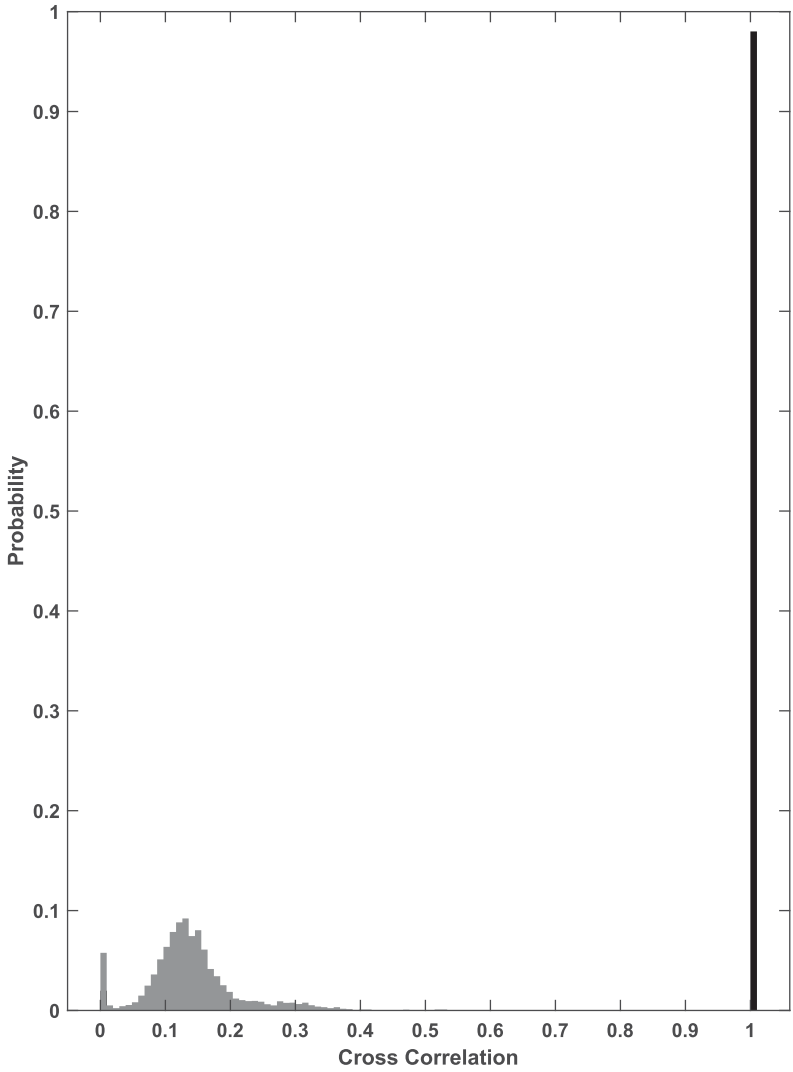

Figure 4: Histogram of magnitudes of elements in the cross-correlation matrix. Off-diagonal elements (between 0 and 0.4) have significantly lower magnitudes than the diagonal elements (peak at 1).

3 Results

Figure 4 shows the cross-correlation between different granule cell patterns at each point in time. The diagonal elements of the cross-correlation matrix

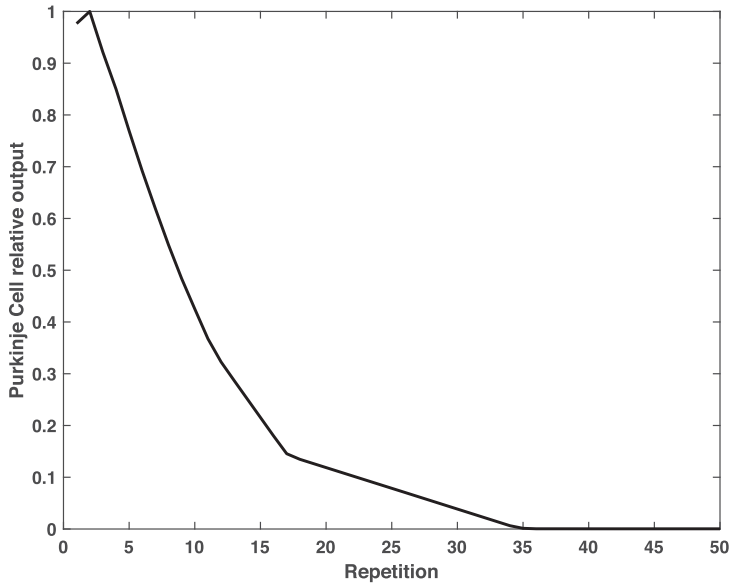

Figure 5: Because of LTD, during training, the Purkinje cell output at the time of the unconditioned stimulus (US) drops to zero.

are much higher than the off-diagonal elements, with no overlap in the distributions. Therefore, there will not be confusion between different patterns, and every time interval has a unique pattern signature. In order to obtain a unique pattern for each time, the granule cells need to be sufficiently different from each other, with sufficiently high firing rates. The mossy fiber inputs are insufficient for this purpose, since patterns are often replicated at different time points. Expansion coding to the granule cells generates a larger variety of independent Poisson-like sequences with a much lower probability (in this case, zero) of confusion of the patterns for two different time intervals. This occurs in part because the time constant of the granule cell EPSC (40 msec in our simulation) allows response to mossy fiber inputs that occur over a finite time interval, therefore expanding potential granule cell patterns beyond the instantaneous mossy fiber pattern set.

Figure 5 shows the rapid convergence of the Purkinje cell output to the desired value during eyeblink conditioning. Fewer than 30 trials are typically required to achieve full suppression of the Purkinje cell outputs. Figure 6 shows the resulting Purkinje cell outputs when presented with the conditioned stimulus (CS) in the absence of the unconditioned stimulus (US) for three different US patterns: single eyeblink, double eyeblink, and a smooth sinusoidal function. The sinusoidal function is trained using LMS as in equation 2.3. It is instructive to compare the eyeblink response

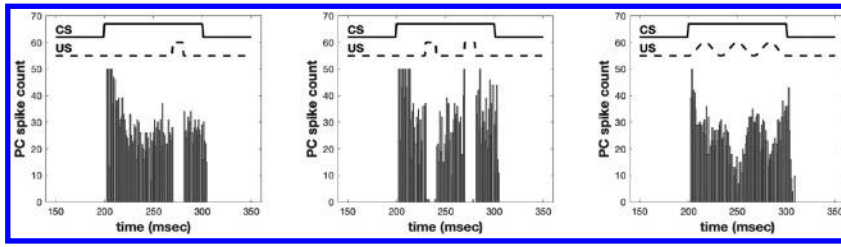

Figure 6: Purkinje cell outputs after training with different US patterns. Left: Single eyeblink conditioning with US present from 270 to 280 msec. Middle: Double eyeblink response with US present from 240 to 250 msec and 270 to 280 msec. Right: Smoothly varying US trained using the LMS algorithm.

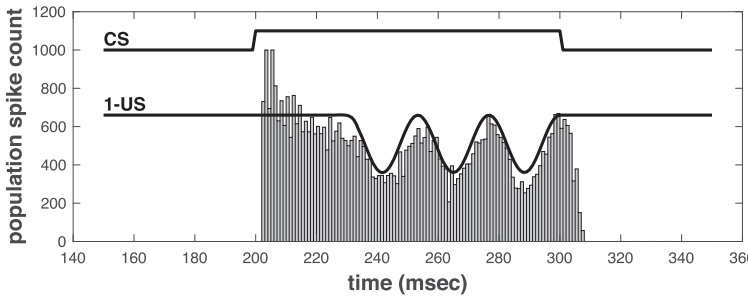

Figure 7: Combined output of 20 Purkinje cells trained by LMS to respond to a smoothly varying US. The combined output population response provides a much better representation of the desired output than any single Purkinje cell.

to in vivo recordings, such as Figure 3 in Kotani, Kawahara, and Kirino (2003), Figure 3 in Jirenhed, Rasmussen, Johansson, and Hesslow (2017), and Figure 5 in Kotani, Kawahara, and Kirino (2006). (Matlab code for this simulation can be downloaded from http://www.sangerlab.net /TimingModelSangerKawato2019.m.)

Because of the inherent variability in Purkinje cell outputs, the representation of the desired sinusoidal function in Figure 6 is not very accurate. However, in the full cerebellum, there would be a population of Purkinje cells to represent these values. Figure 7 shows the summed activity of a population of 20 Purkinje cells, each of which learned to approximate the same sinusoidal function. The population statistics are much smoother than the individual statistics. For the population average to have higher accuracy than its individual elements, the different Purkinje cells must have slightly different responses. This is achieved by adding 1% noise to the synaptic weight change in equation 2.3.

4 Discussion

The very simple LTD/LTP learning algorithm emulated here effectively "deletes" the response to granule cells that tend to be on during the US. However, once deleted, any subset of the deleted set will also lead to a fall in Purkinje cell firing. Thus normalization is necessary for the small numbers of granule cells in our simulation to ensure that random coincidences of pauses in granule cell firing do not automatically lead to low Purkinje cell firing that would be misinterpreted as a conditioned response (CR). This mechanism predicts dense granule cell firing (Badura & De Zeeuw, 2017), since a sparse code will frequently have very few or absent input firing, which would lead to lack of Purkinje cell input that would be mistaken for the decreased firing associated with the CR. Similar to other algorithms, this mechanism is not a model for trace conditioning, since if the CR occurs following the end of the CS, then the granule cells would not be driven by the CS and both granule cells and Purkinje cells would cease firing.

A reasonable analogy is a lock-and-key mechanism. The Purkinje cell synapses are a lock that causes the Purkinje cell to fire for almost all incoming patterns of granule cells. Only when the particular incoming pattern is the key that exactly matches the synapses that have been silenced by LTD does the Purkinje cell stop firing. Normalization (perhaps performed by Golgi cells or other cerebellar interneurons) is essential to ensure that a blank "skeleton" key with little or no granule cell activity would not be able to emulate a truly matching key.

Successful function of the mechanism we propose depends on several details of the network, without which the conditioned response can be incorrect or absent:

1. The pattern of granule cell spike timing during the CS is similar on each repetition of the CS.
2. There is high variation between the spike time patterns of different granule cells.
3. Purkinje cell inputs are normalized.

In order to achieve the first detail, the mossy fiber input needs to have a reliably repeatable pattern for each repetition, there must be no other noise input to the granule cells, and there must be a sufficient intertrial interval that the granule cell membrane potentials can return to their original resting state. In order to achieve the second one, expansion recoding of the mossy fiber input is needed to create a sufficient number of differing spike trains from the mossy fiber input, and the US must occur at a sufficient time interval following onset of the CS that initial transient-correlated responses in the granule cell population have abated. In order to achieve the final detail, there must be either a very large number of granule cells so that in the absence of the US, the mean Purkinje cell EPSP has low variance, or there

must be feedback onto the granule cells that maintains the total granule cell activity approximately constant.

The algorithm proposed here shares important features with prior timing algorithms based on extraction of information from time-varying population responses to the CS input. Tripp and Eliasmith (2006) show that arbitrary output patterns can be computed based on apparently random input patterns similar to those used in our simulations, but they did not implement a cerebellar-like learning rule, and although their results depend on reliable spike timing within the patterns, they do not discuss or simulate mechanisms that permit such timing. Medina et al. (2000) provide a detailed simulation of cerebellar circuitry that estimates temporal patterns as linear combinations of the granule cell patterns. Repeatable patterns of granule cell average firing rates (but not precise spike timing) are induced by variations in network properties within the cerebellar granule and molecular layers. Yamazaki and Tanaka (2007b) demonstrate a spiking neural model with random interconnectivity between granule and Golgi cells that leads to a repeatable but random pattern of firing rates, and they show that a spike-timing-dependent plasticity rule at the parallel fiber to Purkinje cell synapse leads to the ability to learn time intervals in a delay conditioning task. The major difference from the work presented here is that these prior models depend on Purkinje cells detecting (random or known) temporal patterns of spike rates but not the spikes themselves (Rössert et al., 2015). Therefore, the temporal precision of such models is limited because determination of a spike rate requires the generation of multiple spikes over time and cannot respond at the millisecond level of precision. For example, rate-dependent models cannot generally model the ability of Purkinje cells to respond to two different US timings (Jirenhed et al., 2017), whereas we have shown that our model can yield both multiple responses as well as patterned responses at precise intervals (see Figure 6).

Although the granule cell spike trains are repeatable, they appear to have Poisson statistics. A simple rate code that looks at average firing but ignores the temporal pattern would identify the average spatial pattern of activity on the mossy fibers, and this could potentially confuse different conditioned stimulus inputs. By responding to the precise pattern of spikes, the Purkinje cell has the ability to recognize not only the pattern of the CS but the timing as well. Thus, the temporal pattern of spikes on the granule cells identifies both the what and the when of the incoming input data stream.

The model presented here is not intended to be a complete model of cerebellar function or the behavior of eyeblink delayed conditioning tasks. For instance, known phenomena, including the effect of interstimulus interval on learning, extinction of learned eyeblink responses, eligibility traces, and changes in amplitude and reliability, are not modeled (Bareš et al., 2019). The possibility that Purkinje cells have intrinsic time discrimination properties is not modeled (Johansson, Jirenhed, Rasmussen, Zucca, & Hesslow, 2014). The time intervals chosen (100 msec CS with ISIs of 40 or

70 msec) are not intended to be representative of the values seen in eyeblink conditioning; rather, they are intended as examples of high-precision timing responses that can be achieved by this mechanism. Our purpose is to demonstrate the feasibility, precision, and capability of this previously undescribed mechanism without proposing that it is the sole explanation for the complexity of observed learning behaviors.

This model depends critically on the presence of repeatable spike patterns in response to repeatable inputs. Although we believe that individual cells do not have true random effects, there are sufficient numbers of inputs to many cells in the central nervous system that truly repeatable spike patterns may not occur. Despite this concern, there is emerging evidence of specific instances in which repeatable patterns have been found. Our results suggest that whenever this occurs, whether within or outside the cerebellum, there is the potential ability to identify and respond to precise time intervals identified by the specific patterns of spikes that occur over the population at each time. Therefore, this mechanism has the potential to form a more widespread interval timer that could be used for synchronization, sequence generation, recognition and matching of intervals in sensory data, and production of rhythmic sequences. It is tempting to speculate that such a mechanism could be used to fill in the gaps between successive peaks in the theta rhythms generated by thalamus that are thought to provide a global synchronization signal. This would allow the relatively low-frequency theta rhythm to provide a global clock that could be subdivided locally to provide a high-resolution synchronization signal suitable for sensory-motor responses of animals with large bodies and variable peripheral transmission delays.

Acknowledgments

Support for this project was provided by Riken AIP, ATR, and the USC Department of Biomedical Engineering.

References

Alstrøm, P., Beierholm, U., Nielsen, C. D., Ryge, J., & Kiehn, O. (2002). Reliability of neural encoding. *Physica A: Statistical Mechanics and Its Applications*, *314*(1–4), 61–68.

Attwell, P. J., Ivarsson, M., Millar, L., & Yeo, C. H. (2002). Cerebellar mechanisms in eyeblink conditioning. *Annals of the New York Academy of Sciences*, *978*(1), 79–92.

Badura, A., & De Zeeuw, C. I. (2017). Cerebellar granule cells: Dense, rich and evolving representations. *Current Biology*, *27*(11), R415–R418.

Bareš, M., Apps, R., Avanzino, L., Breska, A., D'Angelo, E., Filip, P., . . . Lusk, N. A. (2019). Consensus paper: Decoding the contributions of the cerebellum as a time machine. From neurons to clinical applications. *Cerebellum*, *18*(2), 266–286.

Beylin, A. V., Gandhi, C. C., Wood, G. E., Talk, A. C., Matzel, L. D., & Shors, T. J. (2001). The role of the hippocampus in trace conditioning: Temporal discontinuity or task difficulty? *Neurobiology of Learning and Memory*, *76*(3), 447–461.

Braitenberg, V. (1967). Is the cerebellar cortex a biological clock in the millisecond range? In C. A. Fox & R. S. Snider (Eds.), *Progress in brain research* (Vol. 25, pp. 334–346). Amsterdam: Elsevier.

Buhusi, C. V., & Meck, W. H. (2005). What makes us tick? Functional and neural mechanisms of interval timing. *Nature Reviews Neuroscience*, *6*(10), 755.

Buonomano, D. V. (2003). Timing of neural responses in cortical organotypic slices. In *Proceedings of the National Academy of Sciences*, *100*(8), 4897–4902.

D'Angelo, E. (2014). The organization of plasticity in the cerebellar cortex: From synapses to control. In N. Ramnani (Ed.), *Progress in brain research* (Vol. 210, pp. 31–58). Amsterdam: Elsevier.

Gerwig, M., Kolb, F., & Timmann, D. (2007). The involvement of the human cerebellum in eyeblink conditioning. *Cerebellum*, *6*(1), 38.

Halverson, H. E., Khilkevich, A., & Mauk, M. D. (2018). Cerebellar processing common to delay and trace eyelid conditioning. *Journal of Neuroscience*, *38*(33), 7221–7236.

Hires, S. A., Gutnisky, D. A., Yu, J., O'Connor, D. H., & Svoboda, K. (2015). Low-noise encoding of active touch by layer 4 in the somatosensory cortex. *Elife*, *4*, e06619.

Hopfield, J. J., & Brody, C. D. (2001). What is a moment? Transient synchrony as a collective mechanism for spatiotemporal integration. In *Proceedings of the National Academy of Sciences*, *98*(3), 1282–1287.

Ivry, R. B., & Spencer, R. M. (2004). The neural representation of time. *Current Opinion in Neurobiology*, *14*(2), 225–232.

Izhikevich, E. M. (2003). Simple model of spiking neurons. *IEEE Transactions on Neural Networks*, *14*(6), 1569–1572.

Jirenhed, D.-A., Rasmussen, A., Johansson, F., & Hesslow, G. (2017). Learned response sequences in cerebellar Purkinje cells. In *Proceedings of the National Academy of Sciences*, *114*(23), 6127–6132.

Johansson, F., Jirenhed, D.-A., Rasmussen, A., Zucca, R., & Hesslow, G. (2014). Memory trace and timing mechanism localized to cerebellar Purkinje cells. In *Proceedings of the National Academy of Sciences*, *111*(41), 14930–14934.

Karmarkar, U. R., & Buonomano, D. V. (2007). Timing in the absence of clocks: Encoding time in neural network states. *Neuron*, *53*(3), 427–438.

Kayser, C., Logothetis, N. K., & Panzeri, S. (2010). Millisecond encoding precision of auditory cortex neurons. In *Proceedings of the National Academy of Sciences*, *107*(39), 16976–16981.

Kim, J. J., Clark, R. E., & Thompson, R. F. (1995). Hippocampectomy impairs the memory of recently, but not remotely, acquired trace eyeblink conditioned responses. *Behavioral Neuroscience*, *109*(2), 195.

Kim, J. J., & Thompson, R. E. (1997). Cerebellar circuits and synaptic mechanisms involved in classical eyeblink conditioning. *Trends in Neurosciences*, *20*(4), 177–181.

Kotani, S., Kawahara, S., & Kirino, Y. (2002). Classical eyeblink conditioning in decerebrate guinea pigs. *European Journal of Neuroscience*, *15*(7), 1267–1270.

Kotani, S., Kawahara, S., & Kirino, Y. (2003). Purkinje cell activity during learning a new timing in classical eyeblink conditioning. *Brain Research*, *994*(2), 193–202.

Kotani, S., Kawahara, S., & Kirino, Y. (2006). Purkinje cell activity during classical eyeblink conditioning in decerebrate guinea pigs. *Brain Research*, *1068*(1), 70–81.

Mainen, Z. F., & Sejnowski, T. J. (1995). Reliability of spike timing in neocortical neurons. *Science*, *268*(5216), 1503–1506.

Masquelier, T. (2013). Neural variability, or lack thereof. *Frontiers in Computational Neuroscience*, *7*, 7.

Medina, J. F., Garcia, K. S., Nores, W. L., Taylor, N. M., & Mauk, M. D. (2000). Timing mechanisms in the cerebellum: Testing predictions of a large-scale computer simulation. *Journal of Neuroscience*, *20*(14), 5516–5525.

Miall, C. (1989). The storage of time intervals using oscillating neurons. *Neural Computation*, *1*(3), 359–371.

Molinari, M., Leggio, M. G., & Thaut, M. H. (2007). The cerebellum and neural networks for rhythmic sensorimotor synchronization in the human brain. *Cerebellum*, *6*(1), 18–23.

Narain, D., Remington, E. D., De Zeeuw, C. I., & Jazayeri, M. (2018). A cerebellar mechanism for learning prior distributions of time intervals. *Nature Communications*, *9*(1), 1–12.

Nolte, M., Reimann, M. W., King, J. G., Markram, H., & Muller, E. B. (2019). Cortical reliability amid noise and chaos. *Nature Communications*, *10*(1), 1–15.

Panzeri, S., Ince, R. A., Diamond, M. E., & Kayser, C. (2014). Reading spike timing without a clock: Intrinsic decoding of spike trains. *Philosophical Transactions of the Royal Society B: Biological Sciences*, *369*(1637), 20120467.

Petersen, R. S., Panzeri, S., & Diamond, M. E. (2001). Population coding of stimulus location in rat somatosensory cortex. *Neuron*, *32*(3), 503–514.

Petersen, R. S., Panzeri, S., & Diamond, M. E. (2002). Population coding in somatosensory cortex. *Current Opinion in Neurobiology*, *12*(4), 441–447.

Raymond, J. L., & Medina, J. F. (2018). Computational principles of supervised learning in the cerebellum. *Annual Review of Neuroscience*, *41*, 233–253.

Roössert, C., Dean, P., & Porrill, J. (2015). At the edge of chaos: How cerebellar granular layer network dynamics can provide the basis for temporal filters. *PLOS Computational Biology*, *11*(10).

Schwartze, M., Keller, P. E., & Kotz, S. A. (2016). Spontaneous, synchronized, and corrective timing behavior in cerebellar lesion patients. *Behavioural Brain Research*, *312*, 285–293.

Shmiel, T., Drori, R., Shmiel, O., Ben-Shaul, Y., Nadasdy, Z., Shemesh, M., . . . Abeles, M. (2005). Neurons of the cerebral cortex exhibit precise interspike timing in correspondence to behavior. In *Proceedings of the National Academy of Sciences*, *102*(51), 18655–18657.

Tripp, B., & Eliasmith, C. (2006). Neural populations can induce reliable postsynaptic currents without observable spike rate changes or precise spike timing. *Cerebral Cortex*, *17*(8), 1830–1840.

Uchida, A., McAllister, R., & Roy, R. (2004). Consistency of nonlinear system response to complex drive signals. *Physical Review Letters*, *93*(24), 244102.

Weiss, C., Bouwmeester, H., Power, J. M., & Disterhoft, J. F. (1999). Hippocampal lesions prevent trace eyeblink conditioning in the freely moving rat. *Behavioural Brain Research*, *99*(2), 123–132.

Widrow, B., & Hoff, M. E. (1960). *Adaptive switching circuits* (Technical Report). Stanford University, Stanford Electronics Labs.

Yamazaki, T., & Tanaka, S. (2007a). The cerebellum as a liquid state machine. *Neural Networks*, *20*(3), 290–297.

Yamazaki, T., & Tanaka, S. (2007b). A spiking network model for passage-of-time representation in the cerebellum. *European Journal of Neuroscience*, *26*(8), 2279–2292.

Yamazaki, T., & Tanaka, S. (2009). Computational models of timing mechanisms in the cerebellar granular layer. *Cerebellum*, *8*(4), 423–432.

Received December 2, 2019; accepted June 23, 2020.